Anisotropy of electrical transport and superconductivity in metal chains of Nb_2Se_3

Rongwei Hu,[1,2] K. Lauritch-Kullas,[3] J. O'Brian,[3] V. F. Mitrovic,[2] and C. Petrovic[1]
[1]*Condensed Matter Physics, Brookhaven National Laboratory, Upton, New York 11973-5000, USA*
[2]*Physics Department, Brown University, Providence, Rhode Island 02912, USA*
[3]*Quantum Design, 6235 Lusk Boulevard, San Diego, California 92121, USA*
(Received 12 December 2006; published 28 February 2007)

In this work we have shown bulk superconductivity and studied the anisotropy in both the normal and superconducting states in the quasi-one-dimensional conductor Nb_2Se_3. Electron-electron Umklapp scattering dominates electronic transport along the direction of Nb metal chains as well as perpendicular to it. The superconducting state is rather anisotropic with possible multiband features.

DOI: 10.1103/PhysRevB.75.064517 PACS number(s): 74.70.−b, 74.25.Bt, 74.62.Bf

I. INTRODUCTION

Recently, there has been continuing interest in the search, discovery, and characterization of materials that exhibit exotic collective electronic phenomena in different bonding and structure types. High T_C cuprates, Sr_2RuO_4, some organic and heavy fermion metals are examples of materials which exhibit low dimensional superconductivity gaps or anisotropic Fermi surfaces.[1–4] The true character of anisotropy is one of the most important questions to be addressed, and in that context quasi-one-dimensional (1D) materials are the extreme examples in nature.[5–8] Transition metal chalcogenides often host quasi-1D conducting electrons due to the existence of metal chains in their crystal structure, where band dispersion along the chain is an order of magnitude larger than dispersion in the direction perpendicular to chains. Intermetallic phases on the selenium-rich side of the Nb-Se phase diagram, such as $NbSe_2$ and $NbSe_3$, are fruitful model materials for the study of low dimensional superconductivity and charge density waves (CDW).[9,10] On the other hand, the niobium-rich side of the Nb-Se phase diagram has been far less explored, with the exception of Nb_3Se_4 which is a superconductor with T_C=2.31 K.[11] In this work we show bulk superconductivity and examine the character of anisotropy in the normal and superconducting states of Nb_2Se_3,[12] a quasi-1D conductor whose normal state electronic transport is dominated by electron-electron Umklapp scattering.[13]

II. CRYSTAL STRUCTURE

Nb_2Se_3 crystallizes in the monoclinic $P_{21/m}$ crystal structure where Nb atoms form two types of infinite metal-metal chains running in the *b*-axis direction: Nb(1) and Nb(2). Interatomic distances in the Nb(1) chain are comparable to those in pure metal (2.97 Å), whereas metal distances in the Nb(2) chain are somewhat longer (3.13 Å).[14] The origin of metal clustering in this crystal structure is due to its main building block, M_2X_6 chains (Fig. 1) which are present in many M_2X_3 metal-clustering transition metal chalcogenides (M=Mo,Se,Ta; X=S, Se).[15] M_2X_6 chains are formed by double edge sharing of MX_4 chains which are in turn formed by edge sharing of ideal MX_6 octahedra. Metal-metal bond formation across the shared octahedral edge in MX_4-type chains causes formation of Nb(2) chains and distortion from ideal octahedral building blocks in Nb_2Se_6 clusters. Electrical transport properties and potential structural instabilities in these systems are governed by the bands formed from the set of unfilled t_{2g} orbitals.

Due to metal clustering in the basic Nb_2Se_6 building blocks, band structure is comprised of flat bands originating from Nb(2)-Nb(2) bonding across the shared edge of the $NbSe_4$ chains and rather dispersive bands formed from x^2-y^2 orbitals along the Nb(1) chain. Nb_2Se_3 is isostructural with Mo_2S_3 where metal-metal distances in both Mo(1) and Mo(2) chains are comparable to those in pure Mo metal. Peierls distortion associated with half-filled t_{2g} block bands due to the oxidation state of Mo atoms [$Mo^{3+}(d^3)$] doubles the unit cell so Mo_2S_3 exhibits CDW transition. On the other hand, there is no CDW formation in Nb_2Se_3 since the oxidation state of Nb atoms is Nb^{3+} (d^2). Consequently, Nb_2Se_3 is a good model material for the study of low dimensional electronic transport along metallic chains down to the lowest temperatures without partial destruction of the Fermi surface due to CDW formation, as is the case in many transition metal oxides and chalcogenides.

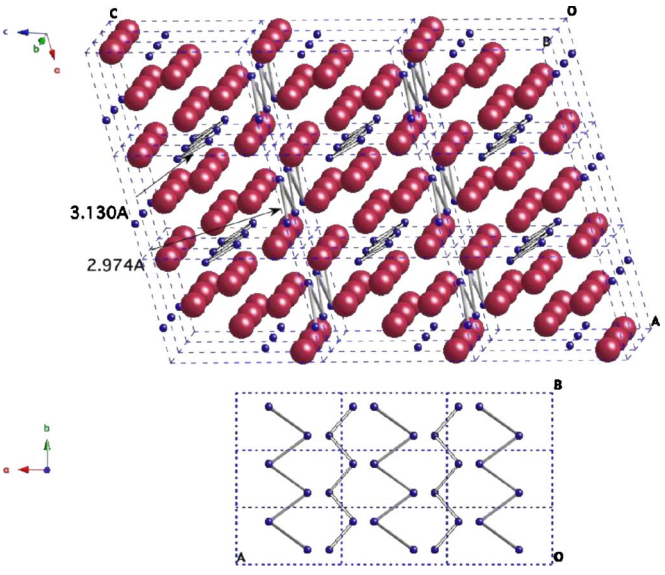

FIG. 1. (Color online) Crystal structure of Nb_2Se_3 (3×3 unit cells shown) and projection onto the *ab* plane showing two types of Nb chains, open and solid bonds. Nb (blue symbol), Sb (red symbol).

III. EXPERIMENT

Powder x-ray patterns were taken at room temperature using a Rigaku Miniflex with CuK_α radiation. The data were collected using 2θ scan in the 10°–90° range. Several different single crystals were oriented by a Laue camera. Electrical contacts were made with Epotek H20E silver epoxy for current along the *b*-axis of the crystal as well as perpendicular to the *b* axis in the *a*-*c* plane (parallel and perpendicular to Nb-Nb chains). The electrical resistivity was measured in a Quantum Design PPMS-9 in the temperature range from 0.4–300 K and up to 90 kOe. The heat capacity was measured using a relaxation technique in the same instrument. The magnetic susceptibility was measured in a Quantum Design MPMS XL-5. The dimensions of the samples were measured by a high precision optical microscope, the Nikon SMZ-800 with 10 μm resolution, and average values are presented. Electrical resistivity, magnetic susceptibility, and heat capacity were reproduced on several independently grown samples from different batches in order to exclude sample dependence.

IV. RESULTS

The synthesis of large single crystals allowed us to study the anisotropy in the normal and superconducting state of Nb_2Se_3. Single crystals of Nb_2Se_3 were grown using a molten metallic flux technique, thus avoiding possible contamination and intercalation of transport agent atoms. [16–18] Crystals grew as thin platelike rods with the long rod axis being the *b* axis of the crystal structure along the Nb-Nb metal chains. Crystal structure parameters of flux grown Nb_2Se_3 crystals are in good agreement with previously published: $a=5.5051(2)$ Å, $b=3.4349(2)$ Å, $c=9.2369(4)$ Å, and monoclinic angle $\beta=130.16(1)°$. The anisotropy in electrical transport for current applied both along and perpendicular to the chain direction at high temperatures is shown in Fig. 2(a). The resistivity of our flux grown samples for current $I\uparrow\uparrow b$ axis (ρ_P) is in good agreement with the data from crystals obtained using a vapor transport technique.[13] Electrical transport for the current perpendicular to the chains, $I\perp b$ axis (ρ_N), is up to an order of magnitude larger, implying less band structure anisotropy than in other linear chain inorganic materials and probably less difference in the band dispersion energy parallel to chains (*b* axis) and perpendicular to it.[19,20] The resistivity decreases with decrease in temperature approaching residual resistivity values below 4 K, $\rho_P=26$ $\mu\Omega$ cm and $\rho_N=105$ $\mu\Omega$ cm. Figures 1(b) and 1(c) show the temperature dependence of the resistivity after subtracting the residual resistivity that has been estimated by the extrapolation of the ρ_P and ρ_N curves to $T=0$.

The clustering of atoms in chains results in the quasi-one-dimensional conduction band model first proposed by Kamimura on the example of $(SN)_x$.[13,21] It was shown that electron-electron Umklapp scattering dominates the electronic transport, whereas electron-phonon and electron-electron normal scattering are negligible.[22] The temperature dependence of the resistivity is given by the power law $\rho-\rho_0=CT^n$ (C=const.). For $k_BT\leqslant(0.1-0.3)\gamma$, where γ is the interchain interaction energy, n takes values of $2\leqslant n\leqslant 3$, and for $k_BT>|\gamma|$, $n=1$. The power law fit of both ρ_P and ρ_N in Fig. 2(b) is possible below $T=15$ K whereas a linear temperature dependence is observed above $T=250$ K. The resistivity for $I\uparrow\uparrow b$ axis takes the form $\rho=\rho_0+CT^n$ with $n=2.1\pm0.1$, $C=(1.40\pm0.02)10^{-8}$ Ω cm/K^n, and resistivity for $I\perp b$ axis has the same temperature dependence with $n=2.07\pm0.04$, $C=(7.1\pm0.7)10^{-8}$ Ω cm/K^n.

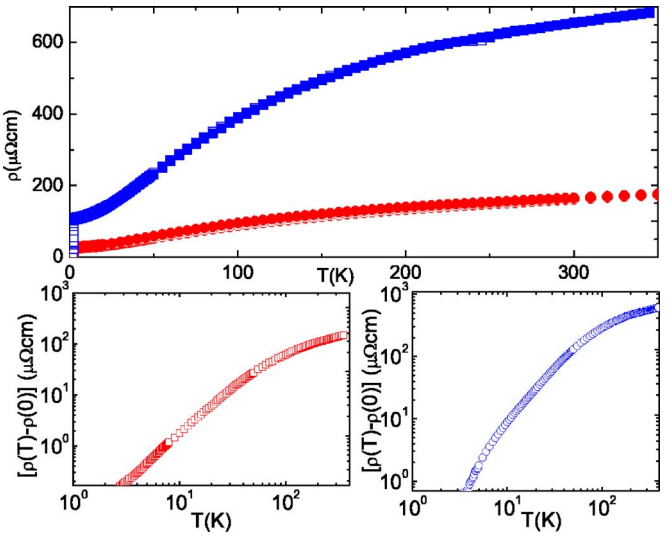

FIG. 2. (Color online) (a) Electrical transport for the current applied parallel (red) and perpendicular (blue) to Nb chains (b axis of the crystal structure) of Nb_2Se_3. (b) ρ-$\rho_0(T)$ for current applied parallel (left) and perpendicular to Nb chains (right).

Low temperature thermodynamic, magnetic, and transport properties are shown in Fig. 3. The jump ΔC at $T_C=2.0$ K in the specific heat and 25% of unsaturated $-1/4\pi$ value in M/H data at the lowest temperature of our measurement (1.8 K) suggest a bulk superconducting transition in Nb_2Se_3. Electrical transport measurements show a somewhat higher transition temperature. For current applied along the chains as well as perpendicular to chains (*b* axis) the onset of the superconducting transition is at $T_\rho^{onset}=2.4$ K. At $T=2.2$ K the transition to the superconducting state for the *b*-axis (ρ_P)

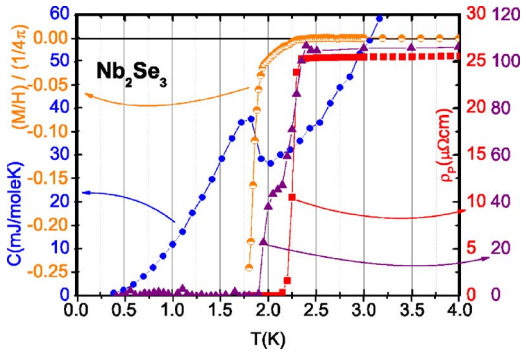

FIG. 3. (Color online) Superconductivity in Nb_2Se_3. Left axis shows thermodynamic properties (heat capacity and magnetization) and right axis shows electrical transport properties for current applied parallel (red symbols) and perpendicular (violet symbols) to Nb chains (b axis of the unit cell).

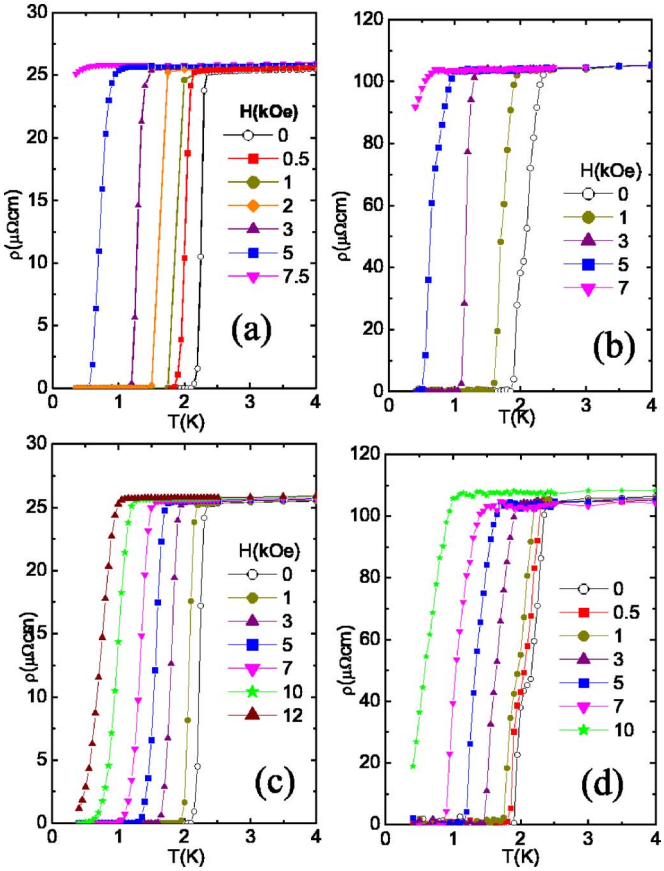

FIG. 4. (Color online) Temperature dependent resistivity for field applied perpendicular (a),(b) and parallel to Nb chains (c),(d), with current applied parallel (a),(c) and perpendicular (b),(d) to Nb chains.

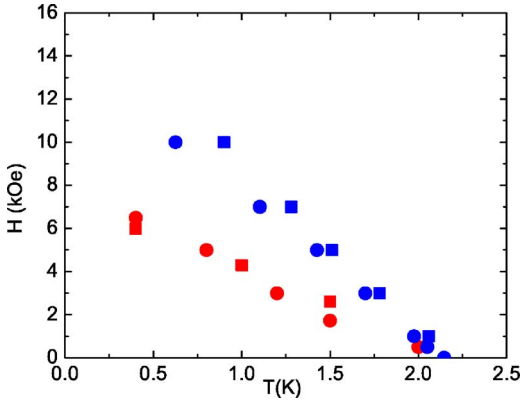

FIG. 5. (Color online) $H_{c2}(T)$ for fields applied perpendicular (red) and parallel to Nb chains (blue symbols) with current applied perpendicular (circles) and parallel to Nb chains (squares).

resistivity is complete whereas resistivity for $I \perp b$-axis (ρ_N) shows a structure and the change of slope. Finally, at bulk $T_C = 2.0$ K, ρ_N is fully superconducting. Magnetic susceptibility M/H is diamagnetic already at T_ρ^{onset} and its magnitude grows towards bulk superconductivity below $T_C = 2.0$ K. By fitting the temperature dependence of the specific heat in the normal state using $C = \gamma T + \beta T^3$, we obtain $C/T = \gamma = 9.96 \pm 0.2$ mJ/mol k^2 and $\theta_D = 223 \pm 3$ K using the relation $\theta_D^3 = (12/5)\ (\pi^4 nR/\beta)$, where R is the gas constant and n is the number of atoms per molecule.

Figure 4 presents temperature-dependent electrical resistivity data for Nb_2Se_3 taken at a variety of applied fields for $H \leqslant 12$ kOe for field applied parallel and perpendicular to Nb chains and for the current running parallel and perpendicular to Nb chains. Two features are evident: there is a suppression of the superconducting phase to lower temperatures for increasing applied field, and there is a negligible magnetoresistivity in the normal state. The decrease of T_C for $I \uparrow \uparrow b$ axis tracks the data well for $I \perp b$ axis for a fixed field direction. On the other hand, suppression of superconductivity is much stronger for $H \perp b$ axis (Nb chains) than for a field applied along the b axis (parallel to Nb chains). A closer look at the temperature dependent resistivity for $I \perp b$ axis reveals a step in the superconducting transition that persists up to 1 kOe. Using these data, $H_{c2}(T)$ curve can be deduced (Fig. 5). We notice an almost linear temperature dependence and relatively large anisotropy of the $H_{c2}(T)$ curve for a magnetic field applied parallel and perpendicular to the Nb chains. There is no sign of saturation down to the lowest temperature of our measurement, 0.4 K.

By extrapolating $H_{c2}(T)$ data to $T = 0$ we get values of $H_{c2}(0) = 7.5$ kOe ($H \perp$ Nb chains) and $H_{c2}(0) = 14$ kOe ($H \uparrow \uparrow$ Nb chains), which is significantly larger. Taken as a whole, the temperature dependence of H_{c2} for Nb_2Se_3 is similar to that found for other quasi-one-dimensional superconductors, for example $TaSe_3$, Nb_3Se_4, and Nb_3S_4. By using $B_{C2}(T) = [\Phi 0/2\pi\xi(T)]$ we obtain coherence lengths $\xi(0) = 203$ Å and $\xi(0) = 153$ Å for a field applied perpendicular and parallel to Nb chains, respectively, a bit shorter than in Nb metal $\xi(0) = 380$ Å.

V. DISCUSSION

Electronic transport in the normal state can be understood in the framework of the theory of Oshiyama and Kamimura.[22] However, our results imply that electron-electron Umklapp scattering is dominant not only along the chain axis of a quasi-one-dimensional metal but also perpendicular to it. The linear resistivity above 250 K and a $\rho \sim T^{2.1}$ temperature dependence of resistivity for both ρ_P and ρ_N below $T = 15$ K, are consistent with the possible range of the chain interaction energy 45 K $\leqslant \gamma \leqslant$ 150 K. We note that the power law temperature dependence of resistivity in vapor transport grown crystals extends up to 40 K, implying a larger value of γ than what we obtained in our work on flux grown crystals. The difference could arise due to the presence of other scattering mechanisms besides electron-electron Umklapp scattering. Alternatively, this may imply that the interchain interaction energy is sensitive to crystalline disorder and imperfections. The flux grown crystals have a higher residual resistivity value $\rho_0 = 26\ \mu\Omega$ cm for the current applied parallel to Nb chains along the b axis of the crystal compared to crystals grown by vapor transport reaction where $\rho_0 = 0.5\ \mu\Omega$ cm.[13]

We turn now to the properties of the superconducting state. Using McMillan's expression[23]

TABLE I. Fundamental parameters of the superconducting state of Nb-Se and Nb-S superconductors. Data on Nb is given for comparison.

	T_C (K)	$\langle a^2 \rangle$	λ
$NbSe_2$	7.1	0.04	0.30
Nb_3S_4	3.78	0.07	0.51
Nb_3Se_4	2.31	0.15	0.51
Nb_2Se_3	2.0	0.16	1.05
Nb	9.25	0.01	1

$$T_C = \frac{\Theta_D}{1.45} \exp\left\{ -\frac{1.04(1+\lambda)}{\lambda - \mu^*(1+0.62\lambda)} \right\} \quad (1)$$

and the value of the Debye temperature from the heat capacity analysis $\theta_D = 223$ K, we estimate the value of the electron-phonon coupling constant $\lambda = 1.05$ assuming the empirical value of pseudopotential $\mu^* = 0.1$. These results put Nb_2Se_3 in the class of the intermediate to strong coupling superconductors. The specific-heat jump $\Delta C/(\gamma T_C) \approx 0.5$ (Fig. 3) is substantially smaller than the mean-field BCS value of 1.43.[24] In the weak-coupling superconductors, the reduced specific heat jump can be interpreted in the terms of the energy gap anisotropy. The effects of an anisotropic energy gap on the thermodynamic properties of the BCS superconductors have been calculated in the seminal work of John Clemm:

$$\Delta C/(\gamma T_C) = 1.426(1 - 4\langle a^2 \rangle), \quad (2)$$

where $\langle a^2 \rangle$, the mean-squared anisotropy, is the average over the Fermi surface of the square of the deviation of the energy-gap parameter from its average.[25] Strong coupling effects and anisotropy in general tend to work in opposite direction and the specific heat jump would be enhanced by strong coupling. This would imply a rather strong anisotropy of the superconducting gap in Nb_2Se_3. Equation (2) therefore gives a rather conservative estimate of $\langle a^2 \rangle = 0.16$. Table I compares the value of electron phonon coupling parameter and the gap anisotropy for several anisotropic superconductors.

Nb_2Se_3 exhibits zero resistivity for current applied along the b axis of the crystal, parallel to Nb chains (ρ_P) at $T = 2.2$ K, whereas the onset of this transition and the transition to a diamagnetic M/H is at $T_\rho^{onset} = 2.4$ K. However, the heat capacity shows a transition to a bulk superconducting state at bulk $T_C = 2.0$ K, where magnetic susceptibility data for M/H shows a dive towards full Meisner effect. These results suggest that the superconductivity of Nb_2Se_3 is a bulk effect below $T_C \sim 2.0$ K and filamentary in nature between T_ρ^{onset} and T_C. Nb_2Se_3 can be regarded as an aggregate of one-dimensional chains that are weakly coupled through Josephson-type junctions since the distance between the Nb atoms in a chain is metallic but the interchain distance exceeds the metallic distance. The temperature dependence of electrical resistivity for current $I \perp b$ axis (ρ_N is perpendicular to Nb chains) is consistent with this interpretation. The onset temperature T_ρ^{onset} is the same for both ρ_P and ρ_N, however ρ_N shows zero resistivity only at bulk T_C and a feature indicating another superconducting transition at $T = 2.2$ K that is visible in applied magnetic field up to 1 kOe. An alternative explanation for this is a small misorientation in the current direction during electrical transport measurement perpendicular to the Nb chains. However, that would imply the presence of two T_C's in two different electronic substructures and negligible interband scattering.[26]

VI. CONCLUSION

In summary, we have showed bulk superconductivity and have investigated the anisotropy in electrical transport properties in the normal and in the superconducting state of Nb_2Se_3. Our results show that Nb_2Se_3 is in the intermediate to large coupling limit of BCS theory with a possible large mean-squared anisotropy of the energy gap on the Fermi surface.

More microscopic measurements such as NMR, neutron scattering, and tunneling experiments would be very useful to quantify the question of possible filamentary superconductivity above bulk T_C or multiband features. We conclude that the Nb_2Se_3 is a promising model system to study superconducting properties in quasi-one-dimensional metallic chain systems.

ACKNOWLEDGMENTS

We thank S. L. Bud'ko, P. C. Canfield, M. Strongin, and Z. Fisk for useful discussions. This work was carried out at the Brookhaven National Laboratory which is operated for the U.S. Department of Energy by Brookhaven Science Associates (DE-Ac02-98CH10886).

[1] J. G. Bednorz and K. A. Muller, Z. Phys. B: Condens. Matter **64**, 189 (1986).
[2] Y. Maeno, H. Hashimoto, K. Yoshida, S. Nishizaki, T. Fujita, J. G. Bednorz, and F. Lichtenberg, Nature (London) **372**, 532 (1994).
[3] T. Ishiguro, K. Yamaji, and G. Saito, *Organic Superconductors*, 2nd ed. (Springer, Berlin, 1998).
[4] C. Petrovic, P. G. Pagliuso, M. F. Hundley, R. Movshovich, J. L. Sarrao, J. D. Thompson, Z. Fisk, and P. Monthoux, J. Phys. Condens. Matter **13**, L337 (2001).
[5] R. C. Morris, R. V. Coleman, and R. Bhandari, Phys. Rev. B **5**, 895 (1972).
[6] N. Kaiser and J. Silk, Nature (London) **324**, 529 (1986).
[7] I. C. McManus, Nature (London) **259**, 426 (1976).
[8] S. L. Bud'ko, V. G. Kogan, and P. C. Canfield, Phys. Rev. B **64**, 180506 (2001).

[9] T. Yokoya, T. Kiss, A. Chainani, S. Shin, M. Nohara, and H. Takagi, Science **294**, 2518 (2001).
[10] A. Perucchi, L. Degiorgi, and R. E. Thorne, Phys. Rev. B **69**, 195114 (2004).
[11] T. Ishida, K. Kanoda, H. Mazaki, and I. Nakada, Phys. Rev. B **29**, 1183 (1984).
[12] K. Igaki and S. Nishine, J. Jpn. Inst. Met. **41**, 843 (1977).
[13] M. H. Rashid and D. J. Sellmyer, Phys. Rev. B **29**, 2359 (1984).
[14] F. Kadijk, R. Huisman, and F. Jelinek, Acta Crystallogr., Sect. B: Struct. Crystallogr. Cryst. Chem. **24**, 1102 (1968).
[15] E. Canadell, A. LeBeuze, M. A. El Khalifa, R. Chevrel, and Myung-Hwan Whangbo, J. Am. Chem. Soc. **111**, 3778 (1989).
[16] Z. Fisk and J. P. Remeika, in *Handbook on the Physics and Chemistry of Rare Earths*, edited by K. A. Gschneider and J. Eyring (Elsevier, Amsterdam, 1989), Vol. 12.
[17] P. C. Canfield and Z. Fisk., Philos. Mag. B **65**, 1117 (1992).
[18] P. C. Canfield and I. R. Fisher, J. Cryst. Growth **225**, 155 (2001).
[19] A. Oshiyama, J. Phys. Soc. Jpn. **52**, 587 (1983).
[20] A. Oshiyama, Solid State Commun. **43**, 607 (1982).
[21] H. Kamimura, A. M. Glazer, A. J. Grant, J. Natsume, M. Schreiber, and A. D. Yoffe, J. Phys. C **9**,291 (1976).
[22] A. Oshiyama and K. Kamimura, J. Phys. C **14**, 5091 (1981).
[23] W. L. McMillan, Phys. Rev. **167**, 331 (1968).
[24] J. Bardeen, L. N. Cooper, and J. R. Schrieffer, Phys. Rev. **108**, 1175 (1957).
[25] J. R. Clem, Ann. Phys. **40**, 268 (1966).
[26] H. Suhl, B. T. Matthias, and L. R. Walker, Phys. Rev. Lett. **3**, 552 (1959).